4th URSI AT-RASC, Gran Canaria, 19 – 24 May 2024

Investigations on Reconfigurable Metasurface Absorber for Wireless Power Transfer

Yugesh Chandrakapure[(1)],Alok Chandra Joshi [(1)],Anand Kumar [(1)], and Debdeep Sarkar[(1)]
(1) Dept. of ECE, Indian Institute of Science, Bengaluru-560012, Karnataka, India

Abstract

In this paper, we have investigated the possibility of wireless power transfer and energy harvesting from a metasurface absorber. A tunable metasurface absorber is developed at 2.58 GHz. The incident waves on the metasurface which are absorbed are harvested for wireless power transfer applications. Furthermore, the effects of the feed location's position on the metasurface are also studied. The prototypes were developed and tested and the results are in good agreement.

1 Introduction

Wireless Power Transfer (WPT) technology enables energy transmission wirelessly, gaining significant attention in industrial and commercial sectors in recent decades [1]. This technology, especially in microwave energy harvesting, has gained prominence across various applications, including healthcare, biomedical systems [2], sensors [3], the Internet of Things (IoT) [4], and wireless communications.

Metasurfaces are two-dimensional structures with periodic arrangements of sub-wavelength resonators that control the amplitude, phase, and polarization of electromagnetic waves [5] for diverse applications such as frequency selective absorption/deflection [6], anomalous reflection [7], and on-air mixing and modulation [8]. Metasurface absorbers, particularly, are popular for electromagnetic shielding, dissipating trapped waves near the resonance frequency of the unit cells to avoid surface reflection.

Although metasurfaces, with large apertures illuminated by electromagnetic waves, are utilized for propagation manipulation, a significant portion of these waves becomes trapped on the metasurface as surface currents, which can be harvested and recycled [9]. Fig. 1 illustrates the concept of energy harvesting through wireless power transfer, where the metasurface absorber operates in absorptive ('ON') and reflective ('OFF') modes based on its bias state. The incident EM waves on the metasurface are trapped and recycled through a power management circuit to harvest its energy which would otherwise have been lost.

In this work, we have developed a transmissive/reflective absorber at 2.58 GHz and studied the possibility of energy harvesting and wireless power transfer through the developed metasurface. In the study, We have shown that a higher surface current flows through the metasurface during the absorption ('OFF') state as compared to its reflection ('ON') state, and when a SMA port is introduced on

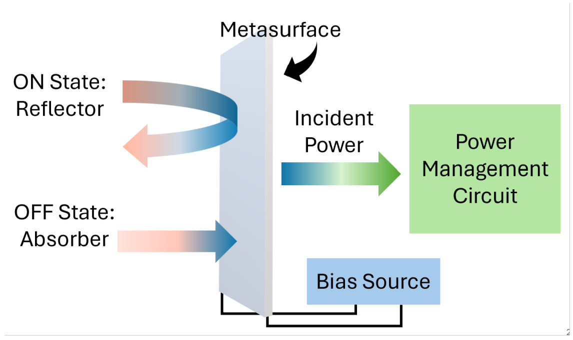

Figure 1. Conceptual representation of energy harvesting and WPT from reflecting/absorbing metasurface.

the metasurface a higher $|S_{21}|$ is observed in the OFF state vs ON state. Further analysis is performed on the port location on the metasurface for a higher reception capability. A prototype is developed as well and the performed analysis has been verified via rigorous measurements.

2 Metasurafce Design

The metasurface's unit cell design, shown in Fig. 2, consists of quarter metallic square rings along the corners which are connected to a circular ring at the center along the diagonals through PIN diodes (NXP BAP64-03) [10]. These rings are imprinted on a grounded dielectric substrate (FR-4, ε_r = 4.4) of thickness 1.6 mm as shown in Fig. 2. The PIN diodes offer a series inductance (L_s) and capacitance (C_{OFF}) when operated under reverse bias (or the 'OFF' state) and a series inductance (L_s) and resistance (R_{ON}) when operated under forward bias (or the 'ON' state) [11]. The unit cell simulation is in CST Microwave Studio for resonance at 2.58 GHz (L_s = 1.68 nH, C_{OFF} = 0.15 pF and R_{ON} = 10 Ω), and the obtained S-parameters and absorption coefficient ($A = 1 - |S_{11}|^2 - |S_{21}|^2$) are shown in Fig. 3. It

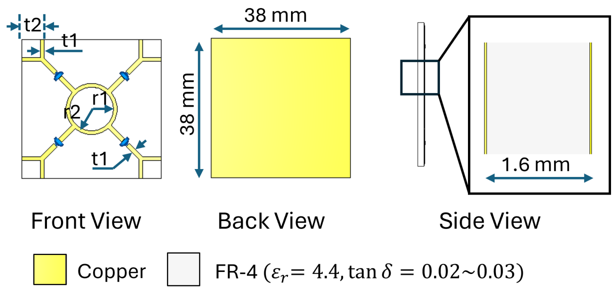

Figure 2. Structure of the Metasurface unit cell

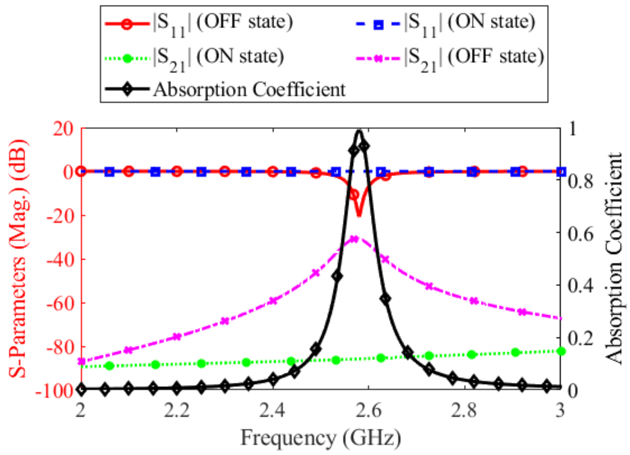

Figure 3. S-parameters and absorption coefficient of the unit cell in Fig. 2

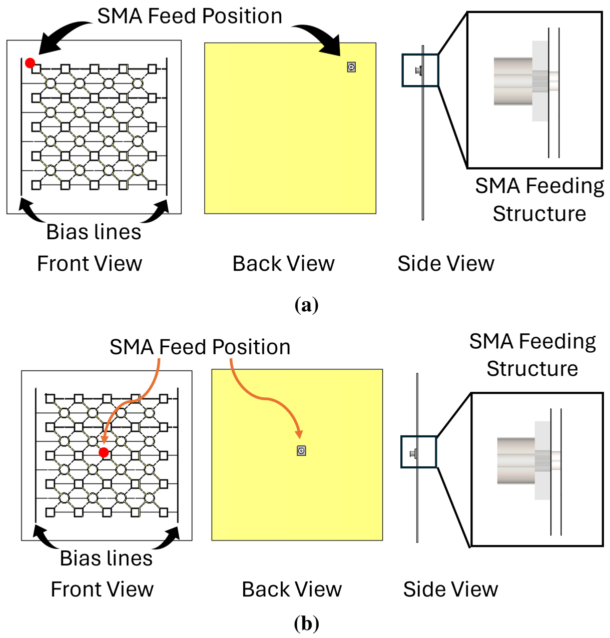

Figure 4. Metasurface design with SMA connector located at (a) top-left corner and (b) center.

is observed that the unit cell acts as a perfect reflector in the ON state and an absorber at 2.58 GHz, the resonance frequency, in the OFF state.

The metasurface is then constructed with a 4×4 array of unit cells in a periodic arrangement as shown in Fig. 4a. To bias the PIN diodes, two vertical metallic patches are imprinted where the bias line on the left is connected to its p-side via the circular rings, and the bias line on the right is connected to its n-side via the square rings. Isolating inductors of 15 nH (LQG15HZ15NH02D, Murata Electronics [12]) are introduced between the unit cells to prevent RF signal flow from the unit cell to the DC bias source. To harness power from the incident wave on the metasurface, an SMA connector of characteristic impedance (Z_0) of 50 Ω is placed on the metasurface and studied under two different locations: (a) at the top-left corner and (b) at the center. The developed prototype of the metasurface is shown in Fig. 9. For the corner-feed case, a 50 Ω SMA

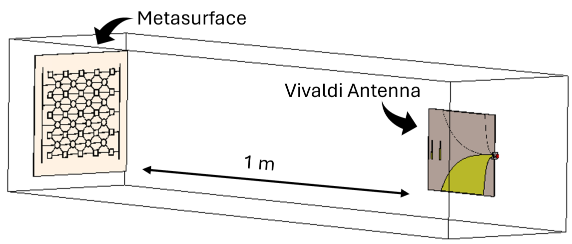

Figure 5. Simulation setup in CST MW Studio for calculation of S-parameters in ON and OFF states

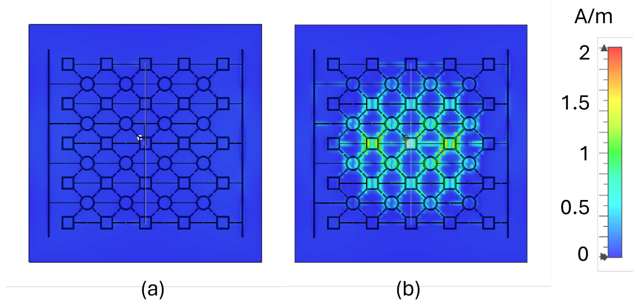

Figure 6. Surface current distribution on the metasurface for normal incidence from Vivaldi antenna in (a) ON state (b) OFF state.

is soldered onto the top-left corner of the square metallic ring, and for the center-feed case, the SMA is affixed to the central square metallic ring, ensuring conformity with the simulated conditions.

3 Results and Discussion

The WPT simulation setup is shown in Fig. 5, where a wideband Vivaldi antenna is placed normally at a distance of 1 m to the metasurface [13]. The power harnessing capability of the metasurface is assessed via simulation and measurement of the S-parameter for both feed locations on the metasurface. For measurements, the bias state of the metasurface is controlled using a DC power supply. In this context, the ON state aligns with a 1 V forward bias, while the OFF state corresponds to a 0 V reverse bias. The S-parameter measurements are obtained through a Vector Network Analyzer (VNA), where port-1 is connected to the Vivaldi Antenna, and port-2 to the SMA connector situated on the rear side of the metasurface. This experimental setup is shown in Fig. 9.

In the ON state, the metasurface functions as a reflector, deflecting a significant portion of incident electromagnetic waves away from its surface. This behavior results in a diminished surface current, leading to a lower S_{21} value compared to the OFF state. On the contrary, when the metasurface is in the OFF state, it works as an absorber where the incoming electromagnetic waves are absorbed, generating a notable surface current. This heightened surface current manifests in an elevated S_{21} value. The surface current distribution for the metasurface is shown in Fig. 6 with a higher current density in the OFF state compared to the ON state and the obtained simulated and measured S_{21} response for both ON and OFF states are shown in Fig. 7a and Fig. 8a

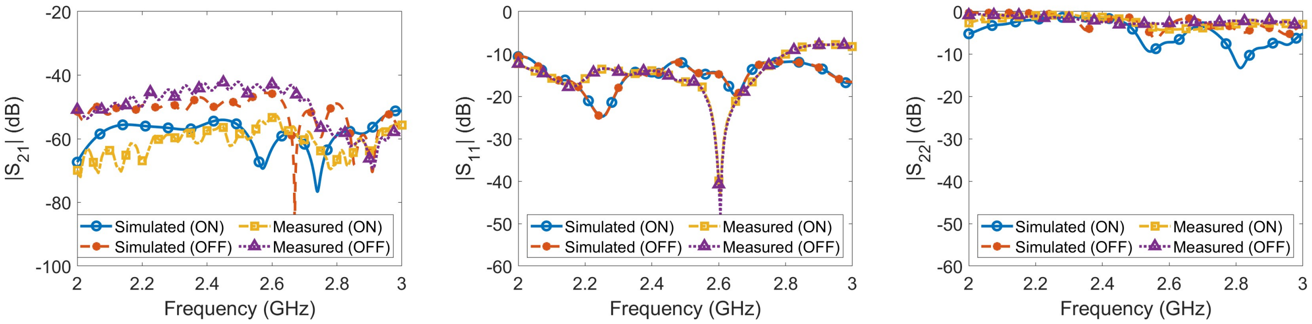

(a) **(b)** **(c)**

Figure 7. Simulated and measured S-parameters of the metasurface for corner located SMA connector: (a) $|S_{21}|$, (b) $|S_{11}|$ and (c) $|S_{22}|$.

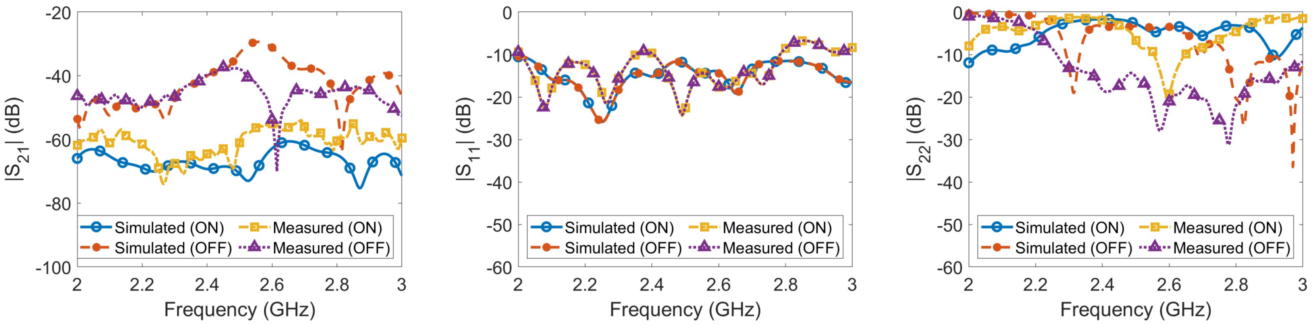

(a) **(b)** **(c)**

Figure 8. Simulated and measured S-parameters of the metasurface for centrally located SMA connector: (a) $|S_{21}|$, (b) $|S_{11}|$ and (c) $|S_{22}|$.

for corner and center feed locations respectively. Essentially, the metasurface's reflective and absorptive characteristics can be adjusted based on its bias state i.e., ON/OFF, influencing the S_{21} response.

In Fig.7b and Fig.8b it can be observed that there is no considerable change in S_{11} in ON and OFF states. This is because there is no change in the surface impedance of the Vivaldi Antenna in these states. In contrast to this, in Fig. 7c, there is a minor change in the S_{22} in ON and OFF states in edge-fed case. This is because in edge-fed case there is a negligible change in the surface impedance caused by surface current. As we have seen that surface current distribution is more at the center compared to the edges in simulation result shown in Fig.6, which is reflected in the considerable change in the S_{22} for the center-fed case as shown in Fig. 8c.

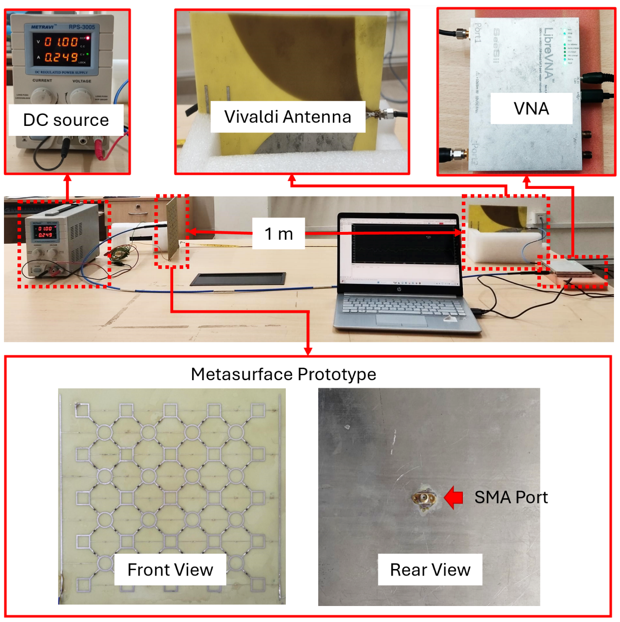

Figure 9. Measurement setup for calculation of S-parameters in ON and OFF states

3.1 Conclusion

This paper investigates the exploration of harnessing wireless power transfer and energy harvesting capabilities from a reconfigurable metasurface absorber. Specifically, a tunable metasurface absorber is crafted to operate at frequency 2.58 GHz. The absorbed incident waves on the metasurface are strategically utilized for wireless power transfer applications, marking a novel approach to energy harvesting. Moreover, the investigation extends to examining the influence of the feed location's positioning on the metasurface, introducing a subtle consideration in optimizing performance. The obtained measurement results exhibit a good correlation with the simulation results. This effort indicates a major step towards the practical implementation of metasurface absorbers in the domain of wireless power transfer and energy harvesting apart from their other benefits such as EM Shielding, RCS reduction, and On-Air frequency Mixing.

Acknowledgements

The authors would like to acknowledge SERB (Science and Engineering Research Board), the Department of Science & Technology (DST), Government of India (GoI) for the technical and financial support through grant no. SRG/2021/000831 and PMRF (Prime Minister's Research Fellowship), Ministry of Education (MoE), GoI for technical and financial support through grant no. TF/PMRF-22-3965.

References

[1] C. R. Valenta and G. D. Durgin, "Harvesting wireless power: Survey of energy-harvester conversion efficiency in far-field, wireless power transfer systems," *IEEE Microw. Mag.*, **15**, 4, Jun. 2014, pp. 108–120, doi: 10.1109/MMM.2014.2309499.

[2] K. Agarwal, R. Jegadeesan, Y.-X. Guo, and N. V. Thakor, "Wireless power transfer strategies for implantable bioelectronics," *IEEE Rev. Biomed. Eng.*, **10**, 2017, pp. 136–161, doi: 10.1109/RBME.2017.2683520.

[3] L. Xie, Y. Shi, Y. T. Hou, and A. Lou, "Wireless power transfer and applications to sensor networks," *IEEE Wireless Commun.*, **20**, 4, Aug. 2013, pp. 140–145, doi: 10.1109/MWC.2013.6590061.

[4] Z. Zhang, H. Pang, A. Georgiadis, and C. Cecati, "Wireless power transfer-An overview," *IEEE Trans. Ind. Electron.*, **66**, 2, Feb. 2019, pp. 1044–1058, doi: 10.1109/TIE.2018.2835378.

[5] A. A. Eteng, H. H. Goh, S. K. A. Rahim, and A. Alomainy, "A review of metasurfaces for microwave energy transmission and harvesting in wireless powered networks," *IEEE Access*, **9**, 2021, pp. 27518–27539, doi: 10.1109/ACCESS.2021.3058151.

[6] N. I. Landy, S. Sajuyigbe, J. J. Mock, D. R. Smith, and W. J. Padilla, "Perfect metamaterial absorber," *Phys. Rev. Lett.*, **100**, 20, 2008, doi: 10.1103/PhysRevLett.100.207402.

[7] S. L. Sun et al., "High-efficiency broadband anomalous reflection by gradient metasurfaces," *Nano Lett.*, **12**, Dec. 2012, pp. 6223–6229, doi: 10.1021/nl3032668.

[8] S. Taravati and G. V. Eleftheriades, "Pure and linear frequency conversion temporal metasurface," *Phys. Rev. A, Gen. Phys.*, **15**, 6, Jun. 2021, Art. no. 064011, doi: 10.1103/PhysRevApplied.15.064011.

[9] F. Erkmen, T. S. Almoneef, and O. M. Ramahi, "Scalable electromagnetic energy harvesting using frequency-selective surfaces," *IEEE Trans. Microw. Theory Techn.*, **66**, 5, May 2018, pp. 2433–2441, doi: 10.1109/TMTT.2018.2804956.

[10] S. Ghosh and K. V. Srivastava, "Polarization-Insensitive Single and Broadband Switchable Absorber/Reflector and Its Realization Using a Novel Biasing Technique," *IEEE Transactions on Antennas and Propagation*, **64**, 8, 2016, pp. 3665–3670, doi: 10.1109/TAP.2016.2565720.

[11] Silicon PIN diode, NXP Semiconductors, Mar 2019, rev. 9. [Online]. Available: https://www.nxp.com/docs/en/data-sheet/BAP64-03.pdf

[12] 15 nH Inductor "LQG15HZ15NH02D" Murata Electronics. Available: $https://www.mouser.in/datasheet/2/281/1/JELF243B_9110-1699596.pdf$

[13] A. Kumar, Easha, D. Sarkar, and G. Banerjee. "A compact quasi-Yagi antenna for FMCW radar-on-chip-based through-wall imaging." *International Journal of Microwave and Wireless Technologies*, 1-13. 2023, doi: 10.1017/S1759078723000235.